Inorganica Chimica Acta, 144 (1988) 193–199

The Tungsten–Tungsten Triple Bond.
XV.* Synthesis, Structure and Reactivity of 1,2-$W_2[CH(SiMe_3)_2]_2(NMe_2)_4$: the Remarkable Inertness of a Sterically-encumbered Tungsten–Amido Complex

M. H. CHISHOLM**, B. W. EICHHORN, K. FOLTING and J. C. HUFFMAN

Department of Chemistry and Molecular Structure Center, Indiana University, Bloomington, Ind. 47405, U.S.A.

(Received July 8, 1987)

Abstract

Addition of 1,2-$W_2Cl_2(NMe_2)_4$(W≡W) to a toluene slurry of $LiCH(SiMe_3)_2$ (2 equiv) results in the formation of 1,2-$W_2[CH(SiMe_3)_2]_2(NMe_2)_4$(W≡W) (**I**) in 79% isolated yield. Compound **I** has been characterized by ^1H and ^{13}C NMR, IR, elemental analysis and single-crystal X-ray diffraction. The molecule exists exclusively in the gauche conformation in solution and in the solid state with W–W = 2.320(1) Å. Compound **I** is very sterically encumbered as evidenced by: (1) large W–W–C angles, 110°, at the disyl ligand; (2) skewing of the NC_2 planes of the NMe_2 ligands off the W–W vector; (3) anomalously large barriers to W–NMe_2 bond rotation in solution; (4) the inertness of **I** towards CO_2 and alcohols. However, compound **I** reacts with acetic anhydride to form 1,2-$W_2[CH(SiMe_3)_2]_2(O_2CMe)_4$(W≡W) (**II**) in 31% isolated yield. Compound **II** has been characterized by ^1H and ^{13}C NMR, IR, and elemental analysis. The mechanistic implications of these studies with regard to alcoholysis and CO_2 insertion reactions of other 1,2-$W_2R_2(NMe_2)_4$ compounds are discussed. Crystal data for 1,2-$W_2[CH(SiMe_3)_2]_2(NMe_2)_4$ at −140 °C: space group $P2_1/n$, $a = 12.555(3)$, $b = 18.699(5)$, $c = 15.214(4)$ Å, $\beta = 95.24(1)°$ and $Z = 4$.

Introduction

We recently reported the activation of various hydrocarbyl ligands in 1,2-$W_2R_2(O\text{-i-Pr})_4$(W≡W) compounds in base-promoted reactions with alkynes [2, 3] phosphines, and amines [4]. For example, the reaction between 1,2-$W_2(CH_2Ph)_2(O\text{-i-Pr})_4$ and quinuclidine (quin), eqn. (1), produces the alkylidyne–hydride complex $W_2(\mu\text{-CPh})(\mu\text{-H})(O\text{-i-Pr})_4(quin)_2$ and one equiv of toluene via a double α-hydrogen activation process.

$$1,2\text{-}W_2(CH_2Ph)_2(O\text{-i-Pr})_4 + 2quin \longrightarrow W_2(\mu\text{-CPh})(\mu\text{-H})(O\text{-i-Pr})_4(quin)_2 + C_6H_5Me \qquad (1)$$

In this and other reactions, alkylidene intermediates are implicated, but attempts to trap these species or detect them spectroscopically have been unsuccessful thus far. We postulated that similar reactions employing alkyl ligands with only one α-hydrogen and no β-hydrogen atoms would yield alkylidene products. One such alkyl group is bistrimethylsilylmethyl or disyl [5]: $[CH(SiMe_3)_2]$.

The 1,2-$W_2R_2(O\text{-i-Pr})_4$ complexes are synthesized from 1,2-$W_2R_2(NMe_2)_4$ precursors by kinetically controlled isopropanolyses [6] according to eqn. (2).

$$1,2\text{-}W_2R_2(NMe_2)_4 + 4i\text{-}PrOH \longrightarrow 1,2\text{-}W_2R_2(O\text{-i-Pr})_4 + 4HNMe_2 \qquad (2)$$

The 1,2-$W_2R_2(NMe_2)_4$ complexes also react with CO_2 [7] and carboxylic anhydrides [8] to form dialkyltetracarbamates, 1,2-$W_2R_2(O_2CNMe_2)_4$, and dialkyltetracarboxylates, 1,2-$W_2R_2(O_2CR')_4$, respectively. These reactions are outlined in eqns. (3) and (4).

$$1,2\text{-}W_2R_2(NMe_2)_4 + 4CO_2 \longrightarrow 1,2\text{-}W_2R_2(O_2CNMe_2)_4 \qquad (3)$$

$$1,2\text{-}W_2R_2(NMe_2)_4 + 4(R'CO)_2O \longrightarrow 1,2\text{-}W_2R_2(O_2CR')_4 + 4R'C(O)NMe_2 \qquad (4)$$

Reaction (3) represents a CO_2 insertion into all four tungsten–amide bonds and reaction (4) is a carboxylate-for-amide metathesis.

We report here the synthesis and characterization of 1,2-$W_2[CH(SiMe_3)_2]_2(NMe_2)_4$ (**I**) and describe its remarkable inertness towards i-PrOH, EtOH and CO_2. The reaction of **I** with acetic anhydride to form 1,2-$W_2[CH(SiMe_3)_2]_2(O_2CMe)_4$ is also discussed.

---

*For Part XIV, see ref. 1.

**Author to whom correspondence should be addressed.

0020-1693/88/$3.50

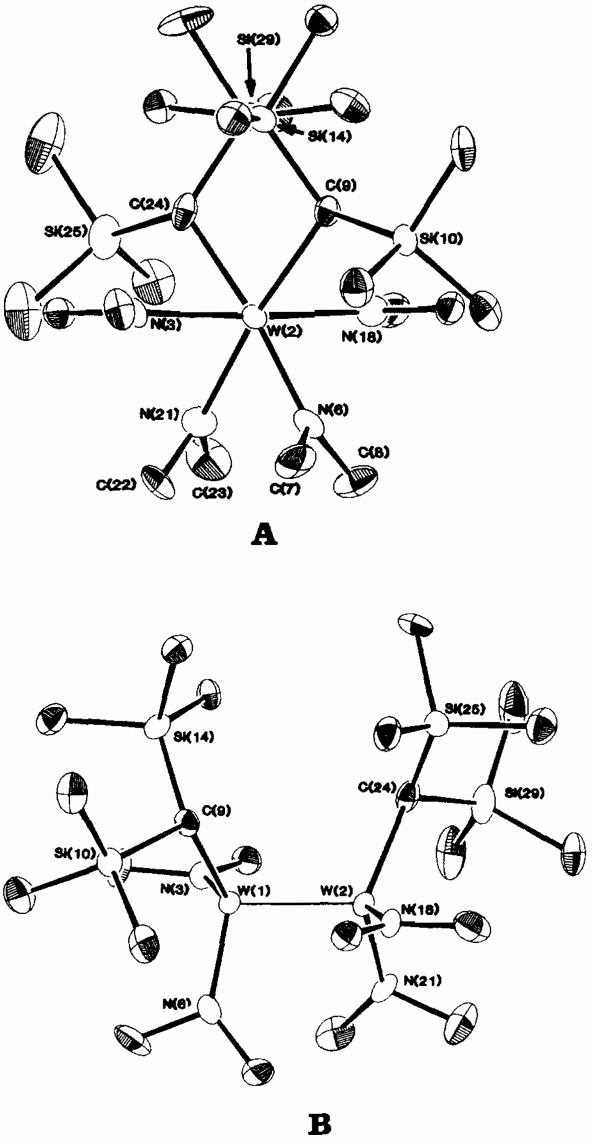

Fig. 1. ORTEP drawings of the 1,2-$W_2[CH(SiMe_3)_2]_2(NMe_2)_4$ molecule, (A) as viewed down the W–W bond showing the gauche conformation of ligands, and (B) side on showing the orientation of the disyl ligand with respect to the W–W vector.

Results and Discussion

Synthesis

Toluene slurrys of $LiCH(SiMe_3)_2$ react cleanly with 1,2-$W_2Cl_2(NMe_2)_4$ at 0 °C to form 1,2-$W_2[CH(SiMe_3)_2]_2(NMe_2)_4$(W≡W) (**I**), according to eqn. (5).

$$1,2\text{-}W_2Cl_2(NMe_2)_4 + 2\,LiCH(SiMe_3)_2 \longrightarrow \mathbf{I} + 2\,LiCl \qquad (5)$$

TABLE I. Summary of Crystallographic Data for $W_2[CH(SiMe_3)_2]_2(NMe_2)_4$

Empirical formula	$C_{22}H_{62}N_4Si_4W_2$
Color of crystal	orange
Crystal dimensions (mm)	0.16–0.20
Space group	$P2_1/n$
Cell dimensions	
Temperature (°C)	–140
a (Å)	12.555(3)
b (Å)	18.699(5)
c (Å)	15.214(4)
β (°)	95.24(1)
Z (molecules/cell)	4
Volume (Å^3)	3556.68
Calculated density (gm/cm^3)	1.615
Wavelength (Å)	0.71069
Molecular weight	864.82
Linear absorption coefficient (cm^{-1})	67.52
Detector to sample distance (cm)	22.5
Sample to source distance (cm)	23.5
Average omega scan width at half height	0.25
Scan speed (°/min)	4.0
Scan width (° + dispersion)	1.8
Individual background (s)	8
Aperture size (mm)	3.0 × 4.0
Two-theta range (°)	6–45
Total no. reflections collected	5044
No. unique intensities	4674
No. $F > 0.0$	4409
No. of $F > 3.0\,P\sigma(F)$	4044
R(F)	0.0390
R_w(F)	0.0385
Goodness of fit for the last cycle	0.935
Maximum delta/sigma for last cycle	0.05

Compound **I** was isolated as red–orange cubes from hexane in 79% yield and has been characterized by ^1H and $^{13}C\{^1H\}$ NMR, IR, elemental analysis, and X-ray crystallography. The crystalline solid is air stable and has a decomposition point of 166–168 °C.

Solid State and Molecular Structure

In the solid state, **I** adopts a gauche conformation as illustrated in Fig. 1. A summary of the crystal data and the atomic positional parameters are given in Tables I and II, respectively. Selected bond distances and angles are given in Table III. The molecular structure is distorted from the typical $M_2X_2Y_4$ ethane-like geometry in the following ways. (1) The W–W–C angle of 110(1)° (ave) is larger than the 99°–104° angle normally observed in $M_2R_2(NMe_2)_4$ compounds [9]. (2) The backbone amido–ligand [N(21) and N(6)] NC_2 planes are not parallel to the metal–metal vector. As a result, the distal NMe_2 methyl carbons lie 0.4(1) Å out of the W–W–N plane. These distortions result from the excessive steric demands of the disyl ligand at the ditungsten center.

TABLE II. Fractional Coordinates and Isotropic Thermal Parameters for $W_2[CH(SiMe_3)_2]_2(NMe_2)_4$

Atom	$10^4 x$	$10^4 y$	$10^4 z$	$10 B_{iso}$
W(1)	5432.8(3)	2264.1(2)	6220.3(3)	12
W(2)	3925.0(3)	2060.0(2)	6959.2(3)	14
N(3)	5228(6)	1640(5)	5192(5)	16
C(4)	6116(8)	1659(7)	4623(7)	24
C(5)	4393(8)	1164(6)	4844(7)	22
N(6)	5260(6)	3284(5)	5960(5)	18
C(7)	5829(11)	3575(6)	5235(8)	32
C(8)	4570(10)	3845(6)	6271(8)	30
C(9)	6881(8)	2019(5)	7097(7)	17
Si(10)	7924(2)	2739(2)	7115(2)	17
C(11)	7466(9)	3596(7)	7543(8)	27
C(12)	8422(10)	2936(7)	6002(8)	29
C(13)	9158(9)	2511(7)	7840(8)	28
Si(14)	7490(2)	1107(2)	6919(2)	17
C(15)	6530(8)	400(6)	6496(7)	21
C(16)	8138(9)	741(6)	8001(7)	23
C(17)	8555(9)	1113(6)	6128(8)	25
N(18)	4181(6)	2611(4)	8037(5)	18
C(19)	3354(11)	2582(7)	8633(8)	31
C(20)	5041(9)	3077(6)	8402(7)	22
N(21)	2814(6)	2424(5)	6099(6)	21
C(22)	2811(9)	2674(7)	5194(8)	29
C(23)	1767(10)	2601(8)	6393(9)	37
C(24)	3754(8)	918(6)	7227(7)	20
Si(25)	2388(2)	543(2)	6899(2)	27
C(26)	2359(11)	−444(8)	7101(10)	46
C(27)	1324(9)	966(7)	7536(9)	34
C(28)	1944(10)	640(8)	5703(10)	42
Si(29)	4286(2)	586(2)	8352(2)	22
C(30)	3247(10)	538(7)	9168(8)	31
C(31)	4841(11)	−341(6)	8279(9)	38
C(32)	5375(9)	1137(7)	8932(8)	27

NMR Studies

In solution, I exists exclusively as the gauche isomer from 22 to 80 °C as determined by ^{1}H and ^{13}C NMR spectroscopy. The ^{1}H NMR spectrum at 22 °C displays two resonances for the diastereotopic $SiMe_3$ groups of the disyl ligands and four NMe_2 methyl singlets. The α-hydrogen of the disyl ligands displays tungsten–hydrogen coupling ($^2J(^{183}W-^1H)$, 14% total satellite intensity) of *ca.* 10 Hz. The room temperature $^{13}C\{^1H\}$ NMR spectrum, Fig. 2, also shows four NMe_2 resonances and two $SiMe_3$ methyl signals with carbon–silicon couplings ($^1J(^{29}Si-^{13}C)$, 5% total satellite intensity) of 49.5 Hz (ave). The signal for the α-carbon atom of the disyl ligand at 47.8 ppm displays tungsten–carbon ($^1J(^{183}W-^{13}C)$, 14% total satellite intensity) and silicon–carbon ($^1J(^{29}Si-^{13}C)$, 9% total satellite intensity) couplings of 78 Hz and 36 Hz respectively. These data are consistent with the solid-state structure of I and, moreover, show that gauche-to-gauche and gauche-to-anti exchange is slow on the NMR scale. Rotation about the tungsten–nitrogen bond [proximal-to-distal NMe_2 methyl exchange] has been monitored by ^{1}H NMR as a function of temperature. One set of NMe_2 methyl resonances has a coalescence temperature (T_c) of 61 °C (334 K) whereas the other set of NMe_2 methyl signals can be estimated to have a T_c of 100–110 °C. The corresponding rotational barriers [10] of 14.8 ± 0.2 and *ca.* 17 kcal mol^{-1} are much larger than those observed in other $M_2R_2(NMe_2)_4$ compounds and are comparable with the rotational barriers observed for the $W_2[M'(M'Me_3)_3]_2(NMe_2)_4$ compounds [M' = Si or Sn]. The rotational barriers ($\Delta G^{\ddagger}$) for I are listed in Table IV together with W–NMe_2 rotational barriers in other 1,2-W_2X_2-

TABLE III. Selected Bond Distances (Å) and Angles (°) for $W_2[CH(SiMe_3)_2]_2(NMe_2)_4$

Atom	Atom	Distance
W(1)	W(2)	2.3199(8)
W(1)	N(3)	1.950(8)
W(1)	N(6)	1.956(9)
W(1)	C(9)	2.203(10)
W(2)	N(18)	1.939(8)
W(2)	N(21)	1.945(8)
W(2)	C(24)	2.189(11)
Si(10)	C(9)	1.877(10)
Si(14)	C(9)	1.897(10)
Si(25)	C(24)	1.878(11)
Si(29)	C(24)	1.884(12)

Atom	Atom	Atom	Angle
W(2)	W(1)	N(3)	103.68(24)
W(2)	W(1)	N(6)	100.25(24)
W(2)	W(1)	C(9)	109.73(28)
N(3)	W(1)	N(6)	114.7(3)
N(3)	W(1)	C(9)	113.7(4)
N(6)	W(1)	C(9)	113.3(3)
W(1)	W(2)	N(18)	104.05(23)
W(1)	W(2)	N(21)	100.54(26)
W(1)	W(2)	C(24)	110.43(28)
N(18)	W(2)	N(21)	115.9(4)
N(18)	W(2)	C(24)	111.9(4)
N(21)	W(2)	C(24)	112.9(4)
W(1)	N(3)	C(4)	113.9(7)
W(1)	N(3)	C(5)	134.7(7)
C(4)	N(3)	C(5)	111.3(9)
W(1)	N(6)	C(7)	117.3(8)
W(1)	N(6)	C(8)	133.7(8)
C(7)	N(6)	C(8)	108.7(10)
W(2)	N(18)	C(19)	116.0(8)
W(2)	N(18)	C(20)	134.4(7)
C(19)	N(18)	C(20)	109.6(10)
W(2)	N(21)	C(22)	133.6(7)
W(2)	N(21)	C(23)	118.8(8)
C(22)	N(21)	C(23)	106.9(10)
W(1)	C(9)	Si(10)	113.3(5)
W(1)	C(9)	Si(14)	114.9(5)
W(2)	C(24)	Si(25)	114.7(6)
W(2)	C(24)	Si(29)	117.3(5)

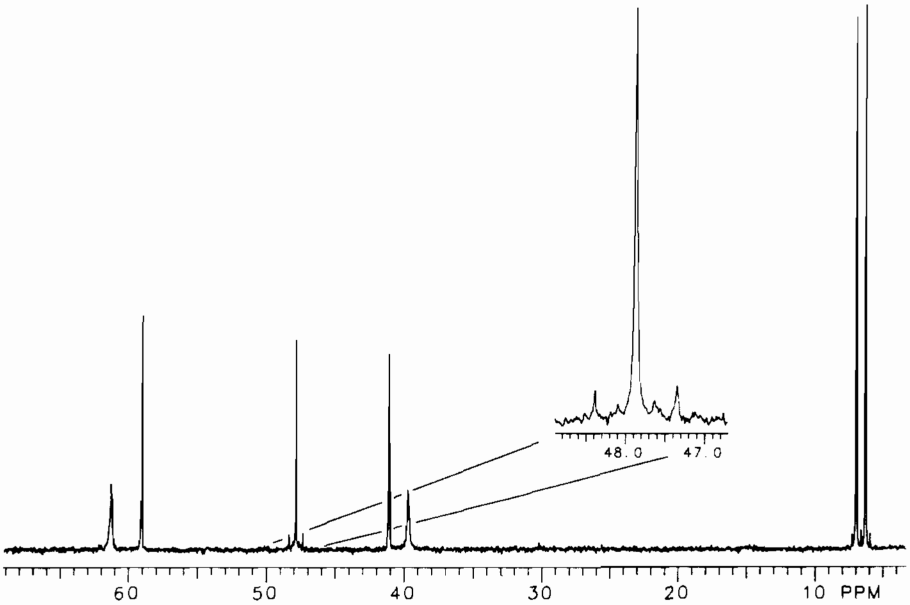

Fig. 2. Room temperature $^{13}C\{^1H\}$ NMR spectrum of 1,2-$W_2[CH(SiMe_3)_2]_2(NMe_2)_4$ recorded in C_6D_6 at 75 MHz. The inset at 47.9 ppm shows the tungsten and silicon satellites on the α-carbon resonance of the disyl ligand.

TABLE IV. Rotational Barriers about W–N Bonds[a]

Compound	$\Delta G^{\ddagger}_{rot}$ (kcal mol^{-1})	Reference
$W_2(NMe_2)_6$	11.2 ± 0.5	17
1,2-$W_2(CH_2SiMe_3)_2(NEt_2)_4$	11 – 14	18
gauche-$W_2[P(t\text{-}Bu)_2]_2(NMe_2)_4$	7.5 ± 0.1 11.3 ± 0.1	11
anti-$W_2[Sn(SnMe_3)]_2(NMe_2)_4$	16.8 ± 0.5	12
gauche-$W_2[CH(SiMe_3)_2]_2(NMe_2)_4$	14.8 ± 0.2 ~17–18	this work

[a]Estimates from coalescence temperature using the Gutowsky–Holm equation: see ref. 10.

$(NMe_2)_4$ compounds [11, 12]. The anomalously large barriers to W–NMe_2 rotation in **I** also reflect the steric pressures of the disyl ligand at the ditungsten center.

Reactions of $W_2[CH(SiMe_3)_2]_2(NMe_2)_4$ (I)

The reactivity of **I** is quite different than that of other 1,2-$W_2R_2(NMe_2)_4$ compounds. For example, 1,2-$W_2(CH_2Ph)_2(NMe_2)_4$ reacts rapidly (t_∞ = 60 min) with i-PrOH (4 equiv) at room temperature [6] to form 1,2-$W_2(CH_2Ph)_2(O\text{-}i\text{-}Pr)_4$, eqn. (2), whereas **I** is inert toward i-PrOH and EtOH even at 80 °C for 5 days. Remarkably, **I** can be recrystallized from EtOH/toluene solvent mixtures (80:20 *v/v*) in high yield. Compound **I** also does not react with CO_2 to form a 1,2-$W_2R_2(O_2CNMe_2)_4$ complex, eqn. (3), in contrast to the rapid CO_2 insertion reactions with other 1,2-$W_2R_2(NMe_2)_4$ complexes [7]. Electronically, the disyl ligand is quite electron releasing* and one must therefore assume that the amido nitrogen atoms of **I** are at least as basic as those in other 1,2-$W_2R_2(NMe_2)_4$ compounds. If alcoholysis occurred by an initial protonation of the amido ligand followed by $HNMe_2$ elimination and RO^- attack, Scheme 1, we suggest that compound **I** should exchange NMe_2 for O-i-Pr or OEt. However, mechanisms proceeding by prior coordination or by four-center transition states would require direct access to the metal center by the R′OH (or CO_2)

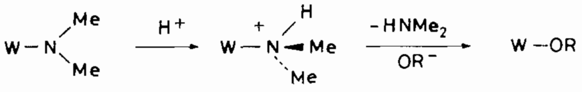

Scheme 1.

---

*The electron releasing capacity of the disyl ligand must be as good or greater than that of $CH_2(SiMe_3)$. For a discussion of organic inductive effects see ref. 13.

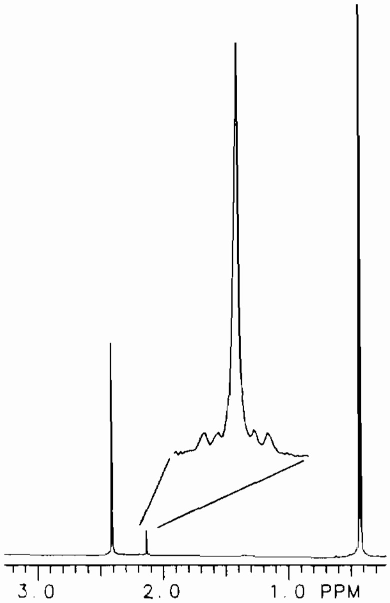

Fig. 3. Room temperature ^1H NMR spectrum of $W_2[CH(SiMe_3)_2]_2(O_2CMe)_4$ recorded in C_6D_6 at 300 MHz. The inset at 2.13 ppm shows the α-hydrogen resonance of the disyl ligand with tungsten and silicon satellites.

reagents. In the present case, such intermediates or transition states would be severely destabilized by steric crowding, which may account for the inertness of **I**.

Compound **I** does react with acetic anhydride in toluene solutions to form the axially coordinated 1,2-$W_2[CH(SiMe_3)_2]_2(O_2CMe)_4$ compound, (**II**) according to eqn. (6). Orange powdery **II** was isolated in 31% yield by sublimation at 110 °C and 10^{-2} Torr. The compound was characterized by ^1H and $^{13}C\{^1H\}$ NMR, IR, and elemental analysis.

$$\mathbf{I} + \text{excess}(CH_3CO)_2O \longrightarrow \mathbf{II} + 4CH_3C(O)NMe_2 \qquad (6)$$

The ^1H NMR spectrum of **II**, shown in Fig. 3, reveals a single disyl α-hydrogen resonance with tungsten and silicon couplings ($^2J(^{183}W-^1H)$, 14% total satellite intensity and $^2J(^{29}Si-^1H)$, 9% total satellite intensity) of 13.5 Hz and 7.6 Hz, respectively. The $^{13}C\{^1H\}$ NMR spectrum shows one type of disyl α-carbon with one-bond and two-bond tungsten couplings ($^1J(^{193}W-^{13}C)$ and $^2J(^{183}W-^{13}C)$, 14% total satellite intensity each) of 121 Hz and 15 Hz respectively. The carboxylate carbon also displays tungsten–carbon coupling ($^2J(^{183}W-^{13}C)$, 24% total satellite intensity) of 3 Hz. These data reliably establish [8] the molecular structure of **II** as an axially coordinated dialkyltetracarboxylate.

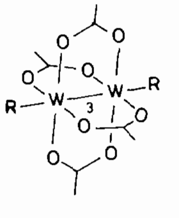

R = $CH(SiMe_3)_2$

II

Conclusions

$W_2[CH(SiMe_3)_2]_2(NMe_2)_4$ (**I**) can be prepared in high yield from the reaction between $LiCH(SiMe_3)_2$ and 1,2-$W_2Cl_2(NMe_2)_4$. In solution and in the solid state, **I** exists exclusively in the gauche conformation. The coordination sphere of the compound is very sterically congested as evidenced by: (1) large W–W–C angles at the disyl ligand, (2) skewing of the NC_2 plane of the amido ligands off of the W–W vectors, (3) anomalously large barriers to $W-NMe_2$ bond rotation, and (4) the inertness of **I** towards i-PrOH, EtOH and CO_2. Compound **I** reacts with acetic anhydride to form the axially coordinated 1,2-$W_2[CH(SiMe_3)_2]_2(O_2CMe)_4$ compound (**II**) in a 31% yield. These studies imply that prior coordination of R′OH and CO_2 may participate in alcoholysis and CO_2-insertion reactions respectively. The same constraints apparently do not apply for the formation of **II**, indicating that acid catalysis may be important in the acid anhydride reactions. Insertions of CO_2 into metal–amide bonds may involve an amine catalyzed sequence: $R_2NH + CO_2 \rightarrow R_2NCOOH$; $M-NR_2 + R_2NCOOH \rightarrow MO_2CNR_2 + HNR_2$. This mechanism is operative for the CO_2 insertion reaction involving $W_2Me_2(NEt_2)_4$ [7b]. Evidently such a mechanism is not operative for **I**. A plausible explanation for the reactivity between **I** and acetic anhydride is that acetic acid, formed by trace amounts of $HNMe_2$ present in solutions of **I**, is a sufficiently strong acid to promote the acid catalyzed sequence shown in eqns. (7a) and (7b) at the sterically protected ditungsten center.

$$HNMe_2 + MeCOCOOMe \longrightarrow MeNCOMe + MeCOOH \qquad (7a)$$

$$MNMe_2 + MeCOOH \longrightarrow MO_2CMe + HNMe_2 \qquad (7b)$$

Experimental

General Procedures

Standard Schlenk procedures and Vacuum Atmospheres Co. Dri-Lab Systems were used for all syntheses and sample manipulations. All solvents were distilled under N_2 from Na/benzophenone and stored in solvent bottles over 4 Å molecular sieves.

The ^1H NMR spectra were recorded in dry and deoxygenated benzene-d_6 on a Varian XL-300 spectrometer at 300 MHz. The data are calibrated against the residual protio impurity in C_6D_6 set at

7.15 ppm and are reported as follows: assignment (chemical shift in ppm, multiplicity, relative intensity, heteronuclear coupling constants). The ^{13}C NMR spectra were recorded in dry and deoxygenated benzene-d_6 on a Varian XL-300 spectrometer at 75 MHz. The data are calibrated against the central C_6D_6 resonance set at 128.0 ppm and are reported as follows: assignment (chemical shift in ppm, heteronuclear coupling constants). Infrared spectra were obtained from KBr pellets using a Perkin-Elmer 283 spectrophotometer and calibrated against the polystyrene absorbance at 1601 cm^{-1}.

Elemental analyses were performed by Schwarzkopf Microanalytical Laboratory, Woodside, N.Y.

Chemicals

The 1,2-$W_2Cl_2(NMe_2)_4$ [14] and $LiCH(SiMe_3)_2$ [15] compounds were prepared by published procedures. Acetic anhydride, EtOH and i-PrOH were purchased and purified by distillation. Bone-dry CO_2 was purchased and used without further purification.

Syntheses

1,2-$W_2[CH(SiMe_3)_2]_2(NMe_2)_4$

A Schlenk reaction vessel was charged with $LiCH(SiMe_3)_2$ (0.994 g, 5.98 mmol) and toluene (15 ml) and cooled to 0 °C producing a milky white slurry. Yellow 1,2-$W_2Cl_2(NMe_2)_4$ (1.84 g, 2.99 mmol) was slowly added to the 0 °C toluene slurry over a 20 min period. The solution slowly turned brown and became homogeneous as the 1,2-$W_2Cl_2(NMe_2)_4$ was added. After the reagents were mixed, the solution was stirred for an additional 1 h at 0 °C followed by 12 h at room temperature. The solvent was removed *in vacuo* from the resulting brown solution and the remaining oily-brown residue extracted into hexane (2 X 8 ml) and filtered through a fine frit. The volume of the orange–brown hexane solution was reduced to *ca.* 5 ml and kept at room temperature. After 2 days, orange–red cubic crystals were isolated by removing the supernatant liquid via cannula, washing the crystals with benzene (2 ml) and drying *in vacuo* (crystalline yield 2.0 g, 79%).

IR (KBr) cm^{-1}: 2950(s), 2880(s), 2860(vs), 2815(s), 2765(s), 1441(m), 1422(w), 1393(vw), 1381(w), 1248(vs), 1151(m), 1138(m), 1121(w), 1035(m), 990(s), 953(s), 940(s), 850 broad (vs), 764(m), 738(vw), 719(vw), 661(s), 606(m), 558(w), 469(w), 344(m).

^{1}H NMR (23 °C, C_6D_6): NMe_2 (4.08, s, 3 H), 3.99, s, 3 H), 2.52, s, 3 H), (2.33, s, 3 H); CH(Si-$Me_3)_2$ (2.55, s, 1 H, $^2J(^{183}W{-}^1H)$ = *ca.* 10 Hz); CH(Si$Me_3)_2$ (0.44, s, 9 H, $^2J(^{29}Si{-}^1H) = 6.0$ Hz), (0.20, s, 9 H, $^2J(^{29}Si{-}^1H) = 6.1$ Hz).

$^{13}C\{^1H\}$ NMR (23 °C, C_6D_6): NMe_2 (61.3), (59.1), (41.4), (39.7); $\underline{C}H(SiMe_3)_2$ (47.9, $^1J(^{183}W{-}^{13}C)$ = 78.3 Hz, $^1J(^{29}Si{-}^{13}C) = 36.2$ Hz); CH(Si$Me_3)_2$ (6.9, $^1J(^{29}Si{-}^{13}C) = 49.8$ Hz), (6.2, $^1J(^{29}Si{-}^{13}C)$ = 49.2 Hz).

Anal. Calc. for $W_2N_4Si_4C_{22}H_{62}$: C, 30.6; H, 7.2; N, 6.5. Found: C, 30.6; H, 7.4; N, 6.2%.

1,2-$W_2[CH(SiMe_3)_2]_2(O_2CMe)_4$

In a Schlenk reaction vessel, 1,2-$W_2[CH(SiMe_3)_2]_2(NMe_2)_4$ (200 mg, 0.232 mmol) was dissolved in toluene (10 ml) and cooled to 0 °C. A large excess of acetic anhydride (2.0 ml) was added to the orange solution via syringe. The color darkened slightly after 10 min and the solution was stirred for an additional 50 min at 0 °C. The orange solution was then warmed to room temperature and stirred overnight during which time no additional color change occurred. The resulting mixture was then evaporated to dryness *in vacuo* leaving an orange–brown powdery residue. The flask was then fitted with a water-cooled cold finger and heated to 110 °C at 10^{-2} Torr. After 24 h, an orange powdery product was isolated from the cold finger (yield 65 mg, 31%).

IR (KBr) cm^{-1}: 2950(m), 2892(m), 2818(vw), 1521(w), 1495(m), 1438(vs), 1382(m), 1350(m), 1255(s), 1248(vs), 1233(s), 1002(s), 941(w), 915(w), 845(vs) broad, 780(m), 769(m), 753(m), 717(w), 660(vs), 628(m), 607(m), 470(m), 337(m).

^{1}H NMR (23 °C, C_6D_6): O_2CMe (2.40, s, 6 H); CH(SiMe$_3)_2$ (2.13, s, 1 H, $^2J(^{183}W{-}^1H) = 13.5$ Hz, $^2J(^{29}Si{-}^1H) = 7.6$ Hz); CH(Si$Me_3)_2$ (0.42, s, 18 H, $^2J(^{29}Si{-}^1H) = 7.4$ Hz).

$^{13}C\{^1H\}$ NMR (23 °C, C_6D_6): $O_2\underline{C}Me$ (181.7, $^2J(^{183}W{-}^{13}C) = 3$ Hz); $\underline{C}H(SiMe_3)_2$ (81.1, $^1J(^{183}W{-}^{13}C) = 121$ Hz, $^2J(^{183}W{-}^{13}C) = 15$ Hz); O_2CMe (20.8); CH(Si$Me_3)_2$ (4.9, $^1J(^{29}Si{-}^{13}C) = 50.5$ Hz).

Anal. Calc. for $W_2Si_4O_8C_{22}H_{50}$: C, 28.6; H, 5.4. Found: C, 28.6; H, 5.4%.

1,2-$W_2[(CH(SiMe_3)_2]_2(NMe_2)_4$ + Alcohols

Attempted alcoholyses were conducted in C_6D_6 solvents in sealed NMR tubes. A typical reaction involved 15 mg of 1,2-$W_2[CH(SiMe_3)_2]_2(NMe_2)_4$ with 5 equiv of EtOH or i-PrOH. The thermolysis reactions (5 days at 80 °C) resulted in small amounts of black precipitate but the only species detectable in solution by ^{1}H NMR spectroscopy were 1,2-$W_2[CH(SiMe_3)_2]_2(NMe_2)_4$ and free alcohol.

1,2-$W_2[CH(SiMe_3)_2]_2(NMe_2)_4$ + CO_2

An extended NMR tube was charged with 1,2-$W_2[CH(SiMe_3)_2]_2(NMe_2)_4$ (26 mg, 0.030 mmol) and benzene-d_6 (0.5 ml) and frozen at −198 °C. Carbon dioxide (4 equiv, 0.12 mmol) was condensed into the NMR tube using a calibrated vacuum manifold. The NMR tube was then sealed with a torch and the reaction monitored by ^{1}H NMR. After 7 days at room temperature, no color change had taken place and only 1,2-$W_2[CH(SiMe_3)_2]_2(NMe_2)_4$ was observed in the ^1H NMR spectrum.

X-ray Structural Determination of 1,2-$W_2[CH(SiMe_3)_2]_2(NMe_2)_4$

General operating procedures and listings of programs have been previously reported [16]. A summary of the crystallographic data is given in Table III. A suitable small crystal was transferred to the goniostat in air and cooled to −140 °C using a gas flow cooling system.

A systematic search of a limited hemisphere of reciprocal space yielded a set of reflections which exhibited monoclinic symmetry and systematic extinctions of $0k0$ for $k = 2n + 1$ and $h0l$ for $h + l = 2n + 1$. The monoclinic space group $P2_1/n$ was chosen and confirmed by successful solution and refinement of the structure.

The structure was solved by a combination of direct methods (MULTAN78) and Fourier techniques and refined by full-matrix least-squares. The hydrogen atoms were evident following refinement of all non-hydrogen atoms. The full-matrix least-squares refinement was completed using anisotropic thermal parameters on all non-hydrogen atoms and isotropic thermal parameters on all hydrogen atoms. No absorption corrections were carried out.

The final difference map contained a few peaks of approximately 1.7 e/Å in the immediate vicinity of the heavy atoms but was otherwise featureless.

Acknowledgements

We thank the National Science Foundation and the Wrubel Computing Center for support. B.W.E. is the 1986/87 Indiana University SOHIO graduate fellow.

References

1 M. H. Chisholm, D. L. Clark, J. C. Huffman and W. G. Van Der Sluys, *J. Am. Chem. Soc., 109*, 6817 (1987).

2 M. H. Chisholm, B. W. Eichhorn and J. C. Huffman, *J. Chem. Soc., Chem. Commun.*, 861 (1985).

3 M. H. Chisholm, B. W. Eichhorn, K. Folting and J. C. Huffman, *Organometallics*, submitted for publication.

4 R. J. Blau, M. H. Chisholm, B. W. Eichhorn, K. Folting and J. C. Huffman, manuscript in preparation.

5 D. E. Goldberg, D. H. Harris, M. F. Lappert and K. M. Thomas, *J. Chem. Soc., Chem. Commun.*, 261 (1976).

6 M. H. Chisholm, B. W. Eichhorn, K. Folting, J. C. Huffman and R. J. Tatz, *Organometallics, 5*, 1599 (1986).

7 (a) M. H. Chisholm, F. A. Cotton, M. W. Extine and B. R. Stults, *Inorg. Chem., 24*, 3214 (1985); (b) M. H. Chisholm and M. W. Extine, *J. Am. Chem. Soc., 99*, 792 (1977).

8 M. H. Chisholm, D. L. Clark, J. C. Huffman, W. G. Van Der Sluys, E. M. Kober, D. L. Lichtenberger and B. E. Bursten, *J. Am. Chem. Soc., 109*, 6796 (1987).

9 M. J. Chetcuti, M. H. Chisholm, K. Folting, D. A. Haitko, J. C. Huffman and J. Janos, *J. Am. Chem. Soc., 105*, 1163 (1983).

10 J. Sandstrom, 'Dynamic NMR Spectroscopy', Academic Press, New York, 1982, pp. 79, 109.

11 M. H. Chisholm, H. T. Chiu, K. Folting and J. C. Huffman, *Inorg. Chem., 23*, 4097 (1984).

12 W. E. Buhro, M. H. Chisholm, K. Folting, J. C. Huffman, *J. Am. Chem. Soc., 109*, 905 (1987).

13 T. H. Lowry and K. S. Richardson, 'Mechanism and Theory in Organic Chemistry', 2nd edn., Harper and Row, New York, 1981, pp. 137–142.

14 M. Akiyama, M. H. Chisholm, F. A. Cotton, M. W. Extine and C. A. Murillo, *Inorg. Chem., 16*, 2407 (1977).

15 N. Wiberg, G. Wagner, G. Muller and J. Rude, *J. Organomet. Chem., 271*(1–3), 381 (1984).

16 M. H. Chisholm, K. Folting, J. C. Huffman and C. C. Kirkpatrick, *Inorg. Chem., 23*, 1021 (1984).

17 N. H. Chisholm, F. A. Cotton, M. W. Extine and B. R. Stults, *J. Am. Chem. Soc., 96*, 4477 (1976).

18 M. H. Chisholm and M. W. Extine, *J. Am. Chem. Soc., 98*, 6393 (1976).